CHEMICAL ENGINEERING TRANSACTIONS
VOL. 116, 2025
A publication of AIDIC
The Italian Association of Chemical Engineering
Online at www.cetjournal.it
Guest Editors: Bruno Fabiano, Valerio Cozzani

ISBN 979-12-81206-18-2; **ISSN** 2283-9216
DOI: 10.3303/CET25116023

Challenges in Modeling Buried Detonation Sources: an Experimental Study

Pierrette Atikpo[a,b,c*], Bart Janssens[a], Charline Fouchier[c], Mark Runacres[b], David Lecompte[a], Delphine Laboureur[c]

[a]Royal Military Academy, Brussels, Belgium
[b]Vrije Universiteit Brussel, Brussels, Belgium
[c]von Karman Institute for Fluid Dynamics, Brussels, Belgium
pierrette.atikpo@mil.be

Buried detonations can release hazardous particulates, leading to adverse impacts on the atmosphere and human well-being. Numerous studies have demonstrated that the explosion source predominantly governs the dispersion of these harmful particles in the near – field. In this paper, air blast and explosive charge mass were investigated as suitable buried detonation source characterization parameters during extensive 32 full – scale explosions of 29 to 50 kg TNT equivalent carried out by the Belgian Defense. The analysis showed that the recorded blast waves were emanating from the detonation cord and not the buried explosives. The excessive depth of burial of the explosives resulted in significant attenuation of their air blast. Given the obsolete nature of the explosives, their charge mass could not be proved to be an effective source characterization parameter. Other parameters such as topsoil maximum height and explosion plume initial height need to be investigated.

1. Introduction

An explosion is a phenomenon resulting from a sudden release of energy (Kinney and Graham, 1985). In a chemical explosion, this energy is highly localized and propagates through the explosive material, transferring energy to adjacent materials. When this propagation occurs through supersonic shock pressure forces, it is termed detonation. Detonation can occur in the air (air detonation), on the ground level (surface detonation) or deep in the ground (buried detonation). Buried detonations are utilized for productive purposes, such as the disposal of obsolete munitions by defense entities, or for destructive purposes in instances of terrorist activities. In the case of productive purposes, it is desirable to achieve complete attenuation of the air blast of the buried explosives, this to ensure the safety of the personnel, equipment and infrastructures around the site. Regardless of their intended use, buried detonations have the potential to release minute harmful particles into the atmosphere, which may have detrimental effects on the environment and human health. Numerous studies have shown that the explosion source primarily controls the dispersion of harmful particles in the near – field (Fouchier et al., 2017; Brown et al., 2004; Kansa, 1997; Church, 1969). The source of an explosion is a highly complex physiochemical process, making it extremely challenging and time – consuming to be rigorously characterized mathematically (Sharon et al., 2012; Brown et al., 2004). Therefore, various simple and effective parameters such as momentum flux, buoyancy flux (Briggs, 1982) and charge mass (Sharon et al., 2012; Cao et al., 2011; Church, 1969) have been employed to characterize it. These parameters are appropriate for characterizing air or surface detonation sources. However, they are not suitable for buried detonation because other critical variables, such as depth of burial, soil type, and soil water content, impact the energy released by the source to the explosion plume. Therefore, the most appropriate parameter for characterizing the energy released by a buried detonation source to the explosion plume is its air blast, as it incorporates the critical variables (Hlady, 2004; Reichenbach et al., 1993a). An air blast is characterized by its peak overpressure, positive impulse, arrival time and positive duration (Kinney and Graham, 1985). The limited number of existing buried detonation semi-empirical models for predicting air blast are complex, lack generalizability across all soil types, and are applicable only to a restricted range of charge masses and depth of burial (Reichenbach et al., 1993a, 1993b).

Paper Received: 9 November 2024; Revised: 11 February 2025; Accepted: 20 March 2025
Please cite this article as: Atikpo P., Janssens B., Fouchier C., Runacres M., Lecompte D., Laboureur D., 2025, Challenges in Modeling Buried Detonation Sources: an Experimental Study, Chemical Engineering Transactions, 116, 133-138 DOI:10.3303/CET25116023

Therefore, the objective of this paper is to investigate the suitable parameter to characterize the energy released by the source to the explosion plume during buried detonations. The investigation has been done experimentally through extensive full – scale explosion of obsolete World War I explosives. The experiments have been conducted by DOVO (Belgian Defense unit in charge of explosive ordnance disposal and destruction).

2. Materials and methods

2.1 Explosives

The experiments were conducted in the DOVO demolition zone (Figure 1a) in Poelkapelle, West Flanders, Belgium. Conventional obsolete World War I explosives were collected by DOVO in fields. These were subsequently cleaned to ensure accurate identification (using an X-ray machine) and to ensure successful detonation. The charge mass was then estimated in TNT mass equivalent. The explosives comprised mixtures of various types, including amatol, trotyl, black powder, ammonal, and PETN. The explosives were subsequently tightly packed inside a rectangular wooden box with dimensions of 60 cm in height, 60 cm in width, and 80 cm in length. An anti – tank mine made of steel and a 250 g cartridge wrapped with detonation cord were added to initiate the explosion (Figure 1b). The mass of the entire load includes that of the explosives and the anti – tank mine. Using an excavator, the assembly was placed in the pit (Figure 1c). The detonation cord was connected to an electric detonator, which was in turn connected to an electric post positioned 15 m from the pit center.

(a) (b) (c)

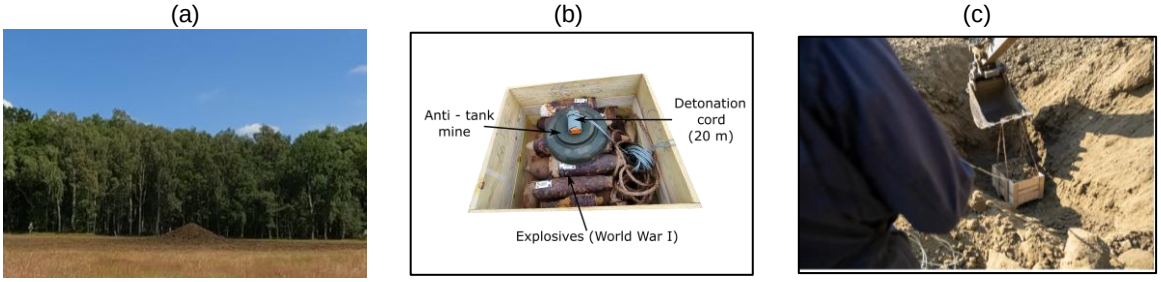

Figure 1: Demolition zone (a), Explosives cleaned and prepared (b) Explosives being deposited in the pit (c)

2.2 Soil type and water content

To characterize the soil type, soil samples were obtained at four distinct depths (0.8 m, 1.2 m, 2.3 m, 3 m). At each depth, 5 kg of soil sample was extracted and divided into three portions: 2 kg was reserved for the dry test, 2 kg for the wet test, and 1 kg as a reserve sample. The soil composition was determined to be 82% sandy (63 µm < particle size < 2 mm), 16% silt (particle size < 63 µm), and 2% gravel (particle size > 2 mm).
The soil water content was quantified using SPEEDY moisture tester. The moisture was not measured for each explosion. It was measured only few times to serve as an indication of all explosions performed during similar weather conditions. It was measured six times (four times for morning explosions and twice for afternoon explosions) between the 5th and the 27th June 2023 during the first experimental campaign. The moisture varied from 10% to 14%.

2.3 Pit and topsoil geometry

Pit dimensions were determined utilizing FARO 3D laser scanner. The explosives were buried in a pit (also termed the explosive chamber), which approximated a conical configuration (Figure 2). The pit had a depth of 3 m, with a minor diameter of 5 m and a major diameter of 6 m (Figure 2b). The pit dimensions were measured before the explosives were deposited. The explosives were subsequently covered with topsoil to a height of 3 m above ground level (Figure 2a). The pit was not scanned for each explosion. It was scanned only once to serve as an indication of all similar explosions. Moreover, the dimensions were measured with ± 1 m variability.

(a) (b)

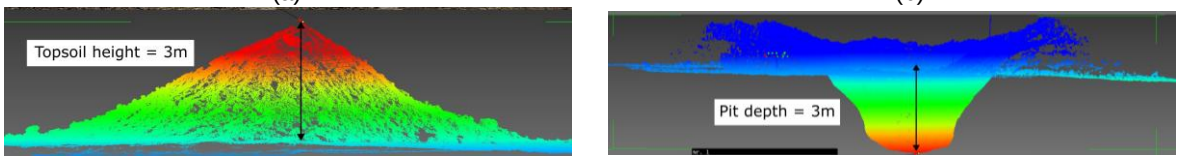

Figure 2: Topsoil (a) and depth of burial (b)

2.4 Experiments and setups

Three experimental campaigns have been conducted. In these experiments, model 137A23 blast pencils with PCB sensors were used. The detonation cord is made of PETN. It has a charge mass of 10g PETN/m and is 20 m long. The shock wave propagates through the detonation cord at 6 000 m/s. The reference time (t=0 ms) corresponds to the ignition of the detonation cord.

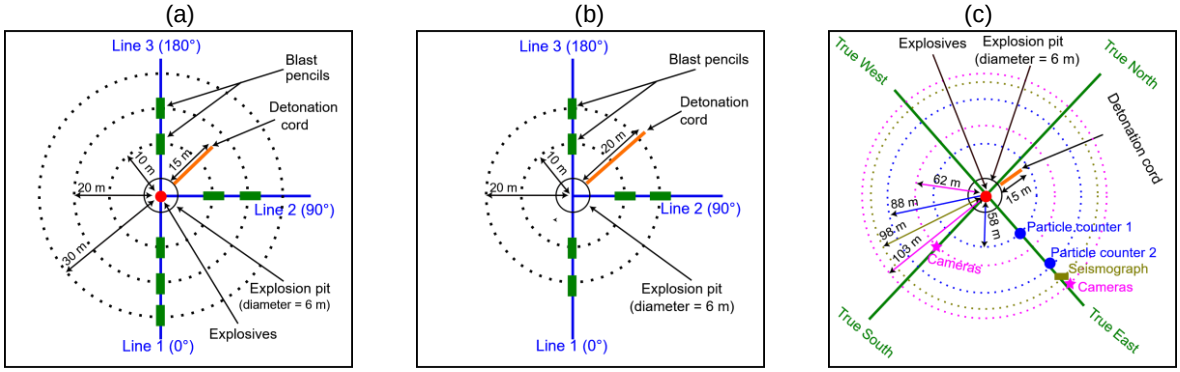

Figure 3: Experimental setup for Experiment 1 (a), Experiment 2 (b) and Experiment 3 (c)

Experimental Campaign 1 : Measurement of explosives air blast

The initial experimental campaign was conducted from June 5 to July 4, 2023. Eleven detonations with charge masses ranging from 29.2 kg to 49.2 kg TNT equivalent were executed. The air blast pressure – time history was recorded with seven blast pencils positioned at a height of 0.9 m, at distances of 10 m, 20 m, and 30 m from the pit center on the lines 0°, 90°, and 180° around the pit. The blast waves were recorded at 5 MHz. The detonation cord was placed on the ground between the 90° and 180° lines, but the exact angle or position of the detonation cord with respect to the lines was not measured. Topsoil motion and early explosion cloud evolution were documented using a Photron SA3 120 K-C2 high – speed camera at 125 Hz to 500 Hz. The camera was positioned approximately 300 m from the explosion center. Figure 3a illustrates the configuration of this initial experimental campaign.

Experimental Campaign 2 : Measurement of detonation cord air blast

On May 24, 2024, the second experiment was executed. Six blast pencils, positioned at a height of 0.9m and distances of 10m and 20m at relative angles of 0°, 90°, and 180° around the pit, were employed to record the air blast pressure – time history at 100 kHz (Figure 3b). Five tests involving solely the detonation cord were performed. In the initial two tests, the detonation cord was placed on the ground surface, with the blast pencil sensor positioned away from the detonation cord. In the subsequent two tests, the detonation cord remained on the ground surface; however, the blast pencil sensor was oriented towards the detonation cord. In the final test, the detonation cord was buried underground. The setup for this second experiment is depicted in Figure 3b.

Experimental Campaign 3 : Measurement of ground vibration

The third experimental campaign was conducted from June 24 to July 09, 2024. Sixteen detonations were performed with charge mass of 33.9 kg to 46.6 kg TNT equivalent. To evaluate the accuracy of explosive charge mass estimation, ground vibration was measured in terms of Peak Particle Velocity (PPV) utilizing a MR3000C SYSCOM seismograph positioned at 98 m true east of the pit center. A high – speed camera (Photron FastCam SA4) operating at 10 kHz–30 kHz was employed to visualize the air blast from the detonation cord. This camera was positioned 103 m from the pit center at a height of 1.4 m. The experimental setup is depicted in Figure 3c.

3. Results and discussions

3.1 Air blast from Experimental Campaign 1: Explosives + detonation cord

A total of 76 blast waves were recorded. Figure 4a gives examples of recorded blast waves.

***Wave strength*:** It was consistently observed that the blast waves at 180° and 90° exhibited greater intensity and arrived earlier compared to the blast waves at 0° (Figure 4a). The peak overpressure at 180° and 90° ranged from 0.8 kPa to 15.1 kPa, while the peak overpressure at 0° varied from 0.3 kPa to 1.2 kPa.

Wave shape: The waves at 180° and 90° demonstrated similar morphology, characterized by a rapid rise and steep peak. In contrast, the waves at 0° exhibited a gradual rise and rounded peak. The detonation cord was positioned between the 180° and 90° lines (Figure 3a), suggesting that the waves at 180° and 90° may originate

from the detonation cord. This hypothesis was corroborated by optical flow analysis (Bhogal and Devendran, 2023) of high – speed recordings. The optical flow analysis revealed a wave – like structure emanating from the detonation cord (Figure 4c).

Peak overpressure vs. charge mass: According to literature (Hlady, 2004; Reichenbach et al., 1993a), a strong positive correlation between the peak overpressure and the buried explosives charge mass should be expected. However, this relationship was not observed in the first experimental campaign (Figure 4b) when considering the mass of the tested explosives. This confirms that the recorded pressure wave originated from the detonation cord rather than the buried explosives.

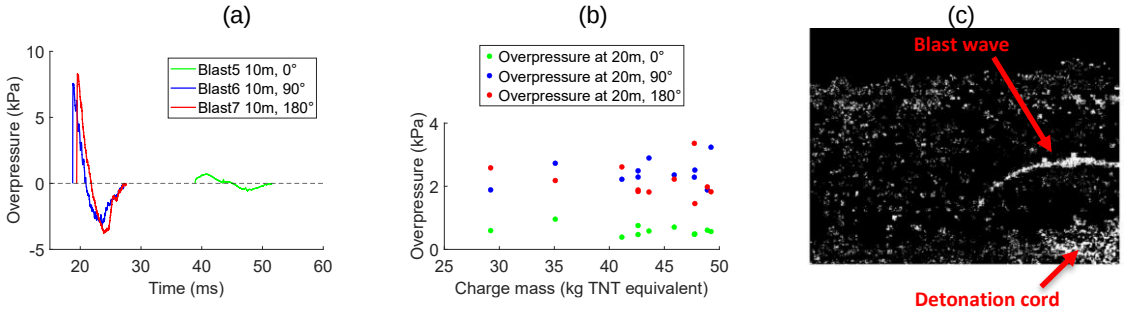

Figure 4: Blast waves (a), peak overpressure vs charge mass (b) and wave visualization using optical flow (c)

3.2 Air blast from Experimental Campaign 2: Detonation cord only

Fourteen blast waves were recorded.

Wave shape: The shape of the waves at 90° and 180° was similar to that observed in Experiment 1 at 90° and 180° (Figure 5a). However, the shape of the waves at 0° is different from that in Experiment 1. This difference can be due to the presence in Experiment 1 of the topsoil (Figure 2a) between the detonation cord and the line 0°. However, the topsoil was absent in Experiment 2.

Wave strength: The recorded peak overpressure at 90° and 180° ranged from 4.1 kPa to 15.3 kPa. This range is consistent with the overpressure at 90° and 180° in Experiment 1 (Figure 5b). The peak overpressure at 0° varied from 1.8 kPa to 2.4 kPa, which is higher than the overpressure at 0° in Experiment 1 (Figure 5c). The higher overpressure at 0° observed in Experiment 2 can be attributed to the topsoil and the length of the detonation cord. In Experiment 1, the presence of the topsoil between the detonation cord and the 0° line could attenuate the blast wave. In Experiment 2, the entire 20 m of the detonation cord was detonated on the ground level, whereas in Experiment 1, only a portion (about 15 m) of the detonation cord was detonated on the ground level. About 5 m was wrapped around the cartridge and buried with the explosives in the ground (Figure 1b).

Burial of detonation cord: When the detonation cord was buried, no blast waves were recorded by the blast pencils at 0°, 90°, and 180° lines.

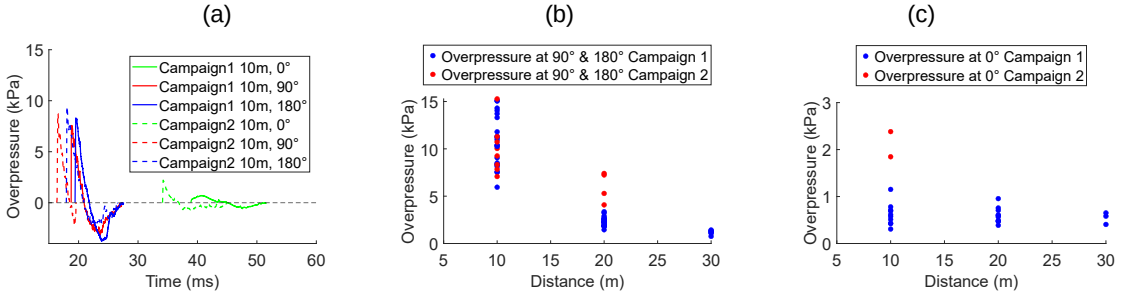

Figure 5: Sample blast waves (a) Overpressure at 90° and 180° (b) Overpressure at 0° (c)

In summary, Experiment 2 indicates that the detonation cord utilized in our experiments emits blast waves. The blast wave shape and strength in Experiment 2 confirm that the blast waves recorded in Experiment 1 at 0°, 90° and 180° (Figure 4a) were emanating from the detonation cord and not the buried explosives. The excessive depth of burial of the explosives resulted in substantial attenuation of their blast effects. Consequently, the air blast could not be utilized as a source characterization parameter in this study. Therefore, an alternative source characterization parameter needs to be investigated.

Theoretical estimation of peak overpressure: The blast pencils on 90° and 180° at 10 m and 20 m with respect to the pit center are at 9.2 m and 14.2 m respectively with respect to the detonation cord center. The

blast pencil on 0° at 10 m with respect to the pit center is positioned at 21.3 m with respect to the detonation cord center. The detonation cord has a total charge mass of 0.254 kg TNT equivalent.

Table 1: Experimental results from Campaign 2 vs theoretical prediction of the peak overpressure

Distance(m)	Peak Overpressure (kPa)					
	Experimental results		Kingery - Bulmash		Kinney - Graham	
	Range	Average	Prediction	Deviation	Prediction	Deviation
9.2 (90°)	7.1 – 15.3	10.9	9	17%	6.3	43%
9.2 (180°)	7.8 – 10.7	9	9	0%	6.3	31%
14.2 (90°)	4.1 – 7.4	6	5.3	12%	3.9	35%
21.3 (0°)	1.8 – 2.4	2.1	3	43%	2.5	20%

Kingery – Bulmash (Kingery et al., 1984) best predicted the average peak overpressure at 90° and 180° with a deviation of 0% to 17% whereas Kinney – Graham (Kinney and Graham, 1985) gave the best prediction at 0° with 20% deviation (Table 1). Several factors such as the virtual source, the source mass type and the position of the blast pencil sensor may explain the discrepancy between the experimental results and theoretical predictions. In this second campaign, the virtual source of explosion was assumed be the center of the detonation cord. The detonation cord is a line mass source while the theoretical models are based on point mass sources. Additionally, the blast pencil was positioned parallel to the detonation cord and directed toward the pit, whereas it is recommended to place it perpendicular to the source to avoid distortion of the blast wave signal during recording.

3.3 Charge mass and ground vibration from Experimental Campaign 3: Explosives + detonation cord

Throughout the experiments, critical variables such as depth of burial, soil type, and soil water content remained largely consistent. Consequently, the charge mass emerged as another potential source characterization parameter. To verify the reliability of the charge mass, a seismograph was employed to measure ground vibration in terms of vertical Peak Particle Velocity (PPV) at 1 kHz. Sixteen ground vibrations were recorded. The collected ground vibrations comprised several waves (Figure 6b and 6c), as corroborated in the literature (Anas et al., 2022; Jayasinghe et al., 2019).

PPV vs. scaled distance : No strong correlation was observed between the PPV and the scaled distance. This can be attributed to the narrow scaled distance range of our experiments which is 27.2 to 30.3 $m/kg^{1/3}$ compared to 2.5 to 25 $m/kg^{1/3}$ in (Anas et al., 2022).

PPV of two similar charge masses: Two detonations with approximately the same mass of 35.9 kg exhibited similar vibration shapes but demonstrated a 24% deviation in their PPV (Figure 6b).

PPV of two different charge masses: Two charges of 34.5 kg and 43.9 kg yielded a PPV of 8.36 mm/s and 8.28 mm/s respectively (Figure 6c).

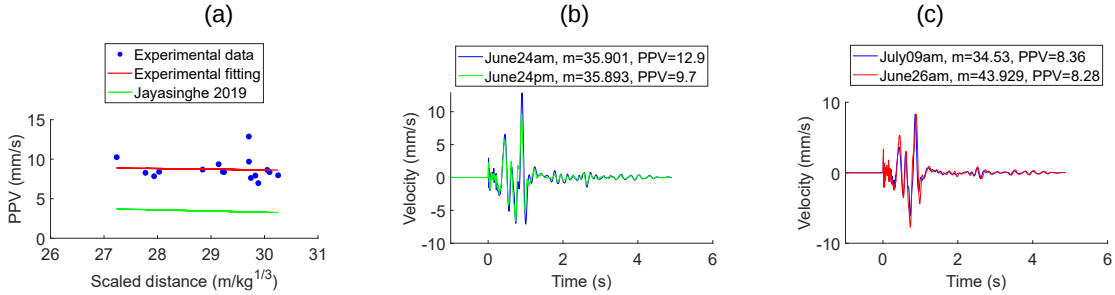

Figure 6: PPV (a), velocity of two similar charge masses (b) and velocity of extreme charge masses (c)

The above discrepancies observed in the PPV can be attributed to the type of explosives, the seismograph sensitivity or the energy effectiveness of the obsolete explosives. Each explosion was composed of different types of mixed explosives. The PPV analysis does not seem sensitive enough to detect variations in the mass of explosives used in our study. To achieve a better velocity reading, one might consider selecting a seismograph with a narrower range or positioning it in closer proximity to the source. Other parameters, such as the maximum height of the topsoil and the initial height of the explosion plume, should be explored.

4. Conclusions

Characterizing the source of full – scale buried detonation presents significant challenges. The analysis indicates that the detonation cord dominates the air blast results. Therefore, in future experiments, it would be prudent to either bury the detonation cord or utilize an electric detonation cord. The excessive depth of burial of the explosives resulted in significant attenuation of their air blast. The charge mass is a crucial parameter for the buried explosion. However, vertical Peak Particle Velocity (PPV) and blast measurements were not effective in characterizing it. Alternative source characterization parameters, such as the maximum height of the topsoil and the initial height of the explosion plume should be explored in future investigations.

Acknowledgments

The authors would like to sincerely thank the following institutions and people for their contribution: DOVO for carrying out the explosions. Adjt Alain Van Hove, from Ballistics Department, for pit dimensions measurement and assistance with detonation cord data collection. Dr. Bogdan Stirbu, from Ballistics Department, for assistance with detonation cord experiment planning. Adjt Renaat Goorts, 1SM Johan Luyckx, 1SG Guillaume Falla, Cpl Gael Maes and Sgt Maxime Demarteau from Department Génie of Amay, for soil data collection and analysis. Professor Alain Muls and Pieterjan De Meulemeester from Signal and Image Centre, for geodesy measurements. Cpt Pascal André, from Department of Mechanical Engineering, Corentin Guinle, Berenger Héméry and Victor Joly from ENSTA – Bretagne, for assistance with blast data collection.

References

Anas, S.M., Alam, M., Umair, M., 2022. Air-blast and ground shockwave parameters, shallow underground blasting, on the ground and buried shallow underground blast-resistant shelters: A review. International Journal of Protective Structures 13, 99–139. https://doi.org/10.1177/20414196211048910

Bhogal, R.K., Devendran, V., 2023. Motion Estimating Optical Flow for Action Recognition : (farneback, horn schunck, lucas kanade and lucas-kanade derivative of gaussian), in: 2023 International Conference on Intelligent Data Communication Technologies and Internet of Things (IDCIoT). Presented at the 2023 International Conference on Intelligent Data Communication Technologies and Internet of Things (IDCIoT), IEEE, Bengaluru, India, pp. 675–682. https://doi.org/10.1109/IDCIoT56793.2023.10053515

Briggs, G.A., 1982. Plume Rise Predictions, in: Lectures on Air Pollution and Environmental Impact Analyses. American Meteorological Society, Boston, MA, pp. 59–111.

Brown, R.C., Kolb, C.E., Conant, J.A., Zhang, J., Dussault, D.M., Rush, T.L., Conway, B.E., Morris, J.W., Touma, J., 2004. Source characterization model (scm) a predictive capability for the source terms of residual energetic materials from burning and/or detonation activities (No. ARI-RR-1384). Strategic Environmental Research and Development Program (SERDP).

Cao, X., Roy, G., Brousseau, P., Erhardt, L., Andrews, W., 2011. A Cloud Rise Model for Dust and Soot from High Explosive Detonations. Propellants Explo Pyrotec 36, 303–309.

Church, H.W., 1969. Cloud rise from high-explosives detonations (No. SC-RR-68-903). Sandia Laboratories, Albuquerque.

Fouchier, C., Laboureur, D., Youinou, L., Lapebie, E., Buchlin, J.M., 2017. Experimental investigation of blast wave propagation in an urban environment. Journal of Loss Prevention in the Process Industries 49, 248–265. https://doi.org/10.1016/j.jlp.2017.06.021

Hlady, S.L., 2004. Effect of Soil Parameters on Land Mine Blast. Presented at the Military Aspects of Blast and Shock (MABS), Bad Reichenhall, Germany.

Jayasinghe, B., Zhao, Z., Teck Chee, A.G., Zhou, H., Gui, Y., 2019. Attenuation of rock blasting induced ground vibration in rock-soil interface. Journal of Rock Mechanics and Geotechnical Engineering 11, 770–778.

Kansa, E.J., 1997. A Time-Dependent Buoyant Puff Model for Explosive Sources (No. UCRL-ID-128733). Lawrence Livermore National Laboratory, Livermore.

Kingery, C.N., Bulmash, G., Laboratory, U.S.A.B.R., 1984. Air Blast Parameters from TNT Spherical Air Burst and Hemispherical Surface Burst. US Army Armament and Development Center, Ballistic Research Laboratory.

Kinney, G.F., Graham, K.J., 1985. Explosive Shocks in Air. Springer Berlin Heidelberg, Berlin, Heidelberg.

Reichenbach, H., Behrens, K., Kuhl, A., 1993a. Airblast environments from buried HE charges (No. UCRL-CR--114890, DNA--001-91-C-0039, 10118533). Defense Nuclear Agency, Washington, U.S.A.

Reichenbach, H., Behrens, K., Kuhl, A.L., 1993b. Approximation Functions for Airblast Environments From Buried Charges (No. E 8/93). Defense Nuclear Agency, Washington, U.S.A.

Sharon, A., Halevy, I., Sattinger, D., Yaar, I., 2012. Cloud rise model for radiological dispersal devices events. Atmospheric Environment 54, 603–610. https://doi.org/10.1016/j.atmosenv.2012.02.050